Inhibition of steel corrosion by calcium benzoate adsorption in nitrate solutions

Article *in* Corrosion Science · February 2005

DOI: 10.1016/j.corsci.2004.06.009

CITATIONS
34

READS
10

4 authors, including:

Guillermo Blustein
Centro de Investigación y Des…
35 PUBLICATIONS **378** CITATIONS

SEE PROFILE

Javier Ernesto Rodríguez Yáñez
Universidad Estatal a Distancia
15 PUBLICATIONS **82** CITATIONS

SEE PROFILE

Available online at www.sciencedirect.com
SCIENCE DIRECT®
Corrosion Science 47 (2005) 369–383
CORROSION SCIENCE
www.elsevier.com/locate/corsci

Inhibition of steel corrosion by calcium benzoate adsorption in nitrate solutions

G. Blustein [a], J. Rodriguez [b], R. Romanogli [a], C.F. Zinola [b,*]

[a] *Centro de Investigación y Desarrollo en Tecnología de Pinturas, CIC-CONICET, Postal Code 1900 La Plata, Argentina*
[b] *Facultad de Ciencias, Laboratorio de Electroquímica Fundamental, Universidad de la República, Libertad No. 2497, Igua 4225, Postal Code 11300, Montevideo, Uruguay*

Received 20 August 2003; accepted 12 June 2004
Available online 22 September 2004

Abstract

The inhibitive properties of calcium benzoate for steel corrosion were studied in sodium nitrate solutions at room temperature. Corrosion parameters of the steel/nitrate and steel/benzoate + nitrate interfaces were obtained from polarisation curves. Adsorption parameters of benzoate on steel in sodium nitrate solutions were determined through changes in the degree of surface coverage by the inhibitor, as a function of concentration, time and adsorption potential. The effect of chloride on the corrosion inhibition of benzoate was analysed exposing the metal in different chloride solution concentrations.

Keywords: Steel; Inhibition; Corrosion; Adsorption; Calcium benzoate

1. Introduction

Steel has found wide applications in a broad spectrum of industries and machinery; however its tendency to corrosion made it not the adequate for exposures in

* Corresponding author. Tel./fax: +598 2 525 0749.
E-mail address: fzinola@fcien.edu.uy (C.F. Zinola).

0010-938X/$ - see front matter © 2004 Published by Elsevier Ltd.
doi:10.1016/j.corsci.2004.06.009

marine atmospheres. The industry of steel and iron goes closely to the incorporation of the proper methodology for metal protection in each application. The use of inhibitors is one of the most widespread strategies to restrain corrosion [1–3]. Two types of corrosion inhibitors are of special interest for protection: adsorption inhibitors in acid corrosion and metal passivation [4]. The inhibitors for acid corrosion have extensive engineering importance in the pickling of scaled metals and in the production of natural gas and oil. Investigations conducted on corrosion inhibition in acid media showed that a great number of effective inhibitors are organic species containing nitrogen, oxygen and/or sulphur [4–6]. The inhibitive action arises from the adsorption to the metal surface of the functional groups contained in the organic compound. It results in a decrease of the anodic and/or cathodic reaction kinetics responsible for the metal corrosion in aggressive environments [5–7]. Many mono- and poly-functional organic inhibitors are being described in the current literature through their efficiencies to corrosion inhibition, as well as their adsorption characteristics [8–18]. A detailed list with the dosage of these inhibitors to restrain metal corrosion can be found in the review by Fontana and Greene [19].

Different electrochemical techniques such as linear polarisation (PC) curves, cyclic polarisation tests, electrochemical impedance spectroscopy and surface scanning with ultra-microelectrodes have been used to envisage the mechanism of corrosion inhibition on various metals [20–22]. From the pioneer works of Bockris et al. [23,24], it has been also shown the importance to include in situ spectroelectrochemical methodologies as complementary tools for the investigation of the inhibitors adsorption.

Benzoate compounds also offer interesting possibilities for corrosion inhibition and are of particular interest because of their safe use and high solubility in water [25–34]. The influence of benzoate concentration, pH and dissolved oxygen on the corrosion of pure annealed iron was studied employing sodium benzoate solutions [24,25,32]. The inhibition effect by benzoate was attributed to the blocking of surface sites in the anodic dissolution by the inhibitor molecule. According to the literature [27,32] the degree of adsorption by benzoate compounds on ferrous metals follows the Langmuir isotherm. Moreover, the adsorption of the inhibitor competes with that of anions such as chloride and sulphate [28].

The corrosion inhibition of carbon steel by blends of gluconate and benzoate and blends of benzoate and acetate was also reported as a new possibility for their use [29,30]. Sodium benzoate and p-substituted benzoic acid derivatives were employed as corrosion inhibitors for aluminium in acid media [31,33,34].

Recently, an increasing interest in the use of organic inhibitors in the field of paint technology grew up during the last decade. Many of these inhibitors were found to improve the anticorrosive behaviour of inorganic pigments [35–39]. Among these inhibitors, the salts formed by benzoic acid and bivalent cations, such as calcium and zinc, have gained acceptance due to the inhibitive properties of the anion [35–37] which may be highlighted by the presence of the cation [40,41]. Moreover, it has been found that metallic benzoates are also useful to reduce "*flash rusting*" in water-borne paints [42].

In this work, the adsorption parameters that characterise the inhibition effects of calcium benzoate on steel are approached by classical electrochemical techniques in sodium nitrate solutions. The influence of chloride is also evaluated through the PCs.

2. Experimental

2.1. Materials and solutions

A three electrode compartment cell was used for the electrochemical and adsorption measurements (cyclic voltammetry, electrochemical adsorption and polarisation curves). The working electrodes were made of SAE 1010 steel rods. They were embedded in parafilm and coated with poly-urethanic paint so as its geometric area resulted in 0.122 cm^2. All the working electrodes were mechanically polished with emery paper up to a 1200 grid and subsequently rinsed in pure water.

The counter electrode was a large-area platinum electrode (approximately 20 cm^2) and the reference electrode a saturated calomel device in a double-fritted glass compartment to avoid chloride diffusion into the main vessel. The supporting electrolyte was prepared with sodium nitrate (99.998% by Merck), the working solutions with the addition of calcium benzoate (lab-prepared with benzoic acid, ammonium hydroxide and calcium nitrate) and/or sodium chloride (99.99% by Merck) with APS Ultra water ($\rho > 18.2\,M\Omega cm$).

2.2. Equipments

The electrochemical experiments were performed using a PGP Radiometer Potentiostat–galvanostat with the Voltamaster 1 software.

Alternatively, the surface morphology of steel, previously subjected to distinct electrolyte solutions for 48 h, was analysed by a Phillips SEM 505 Scanning Electron Microscope coupled with an EDAX OX Prime 10 (energy dispersed form).

The reflectance spectra were recorded with a GBC CINTRA 40/UV–visible spectrometer, which operate between 190 and 1000 nm. Spectra were scanned in the 200–800 nm range.

2.3. Technical methodologies

Before the adsorption and PC experiments, cyclic voltammetry was run at $0.50\,V\,min^{-1}$ between the solvent stability potentials to obtain the electrochemical spectra of steel in the different electrolyte solutions.

2.3.1. Polarisation curves

Linear sweep PCs were obtained by scanning at $0.05\,V\,min^{-1}$ the working electrode in the ±0.10 V range from the open circuit (oc) potential of the steel/electrolyte interface. Corrosion current densities (j_{corr}) and corrosion potentials (E_{corr}) were evaluated from the intersection of the linear anodic and cathodic branches of the

PC as Tafel plots. They were calculated by linear regressions in the ±0.05 V linear ranges from the oc potential with the Voltamaster 1 software.

2.3.2. Adsorption isotherms

The adsorption isotherms were constructed by evaluating the j_{corr} in the presence and in the absence of the inhibitor ($j_{corr,0}$). All measurements were carried out in normally oxygenated solutions without stirring and at room temperature (20 °C).

The surface coverage of the steel electrode by benzoate (θ) in nitrate solutions was determined at different calcium benzoate solution concentrations (C), adsorption times (t_{ads}) and adsorption potentials (E_{ads}). In this method, it is assumed that the inhibitor is homogeneously distributed on the steel surface and only a monolayer is formed on the electrode [48–50]. Thus, on the basis of this consideration, the value of θ is

$$\vartheta = 1 - \frac{j_{corr}}{j_{corr,0}} \tag{1}$$

According to the literature [27,32] the adsorption process of aromatic containing compounds on ferrous metals can obey Langmuir, Temkin or Frumkin isotherms. They were checked in the 10^{-5} M < C < 10^{-1} M range at t_{ads} = 20 min and oc potential. Moreover, in the case of $C = 10^{-2}$ M, t_{ads} was varied from 0 to 60 min. On the other hand, θ values were also evaluated varying E_{ads} from the oc ±0.30 V in $C = 10^{-2}$ M at t_{ads} = 30 min.

2.4. The influence of chloride in solution

The effect of chloride on the inhibition of steel corrosion caused by benzoate was studied following the routines described below:

Routine A

Firstly, benzoate was adsorbed on steel in 0.10 M calcium benzoate + 0.70 M sodium nitrate solution during 30 min at the oc potential. Secondly, the steel surface was put in a solution of 0.10 M benzoate + 0.70 M nitrate containing different concentrations of sodium chloride (0.01, 0.10 and 0.40 M) at the new oc potential for 10 min. Finally, the PC was run in those solutions at 0.05 V min^{-1} within the ±0.10 V domain from the oc potential. From the linear lines the corrosion parameters were determined.

Routine B

Firstly, the steel surface was put in contact with 0.10 M calcium benzoate + 0.70 M sodium nitrate solution during 30 min at the oc potential. Secondly, the passivation of the surface was accomplished at 0.40 V for 10 min in the same solution and thirdly the electrode was put in contact with a solution containing 0.40 M sodium chloride + 0.10 M calcium benzoate + 0.70 M sodium nitrate at the new oc potential also for 10 min. Finally, the PC was run at 0.05 V min^{-1} in the ±0.10 V domain from the oc potential to determine the corrosion parameters.

Routine B was repeated in similar conditions, but without calcium benzoate and in another without solution chloride for comparison purposes.

3. Results and discussion

3.1. Electrochemical and surface characterisation of SAE 1010 steel in the presence of calcium benzoate

The cyclic voltammogram of a SAE 1010 steel surface in oxygen free 0.70 M sodium nitrate run at 0.50 V min^{-1} is shown in Fig. 1. The anodic profile exhibits a complex contour of four peaks with the onset potential of steel oxidation approximately −0.7 V, which corresponds to the formation of a monolayer of ferrous oxide [43]. The first stage of steel oxidation defines an anodic peak at −0.60 V, whereas the formation of the two bulk iron oxides occurs at −0.40 and 0 V, respectively. The fourth peak appeared at approximately 0.25 V, like a hump of the third peak. The passivation of the steel surface in the electrolyte took place from 0.50 to 1.00 V. In the reverse scan, two cathodic peaks were observed at −0.25 V and −0.50 V denoting the reduction of the iron oxides in aqueous 0.70 M sodium nitrate.

In the same figure is depicted the voltammogram of the steel surface in 0.10 M calcium benzoate + 0.70 M sodium nitrate run at 0.50 V min^{-1}. The electrochemical spectrum shows little activation by iron dissolution. Thus, no anodic peak can be clearly seen, but in the reverse scan a cathodic contribution at approximately −0.6 V was observed. This fact shows the inhibitive action of the benzoate layer on iron dissolution.

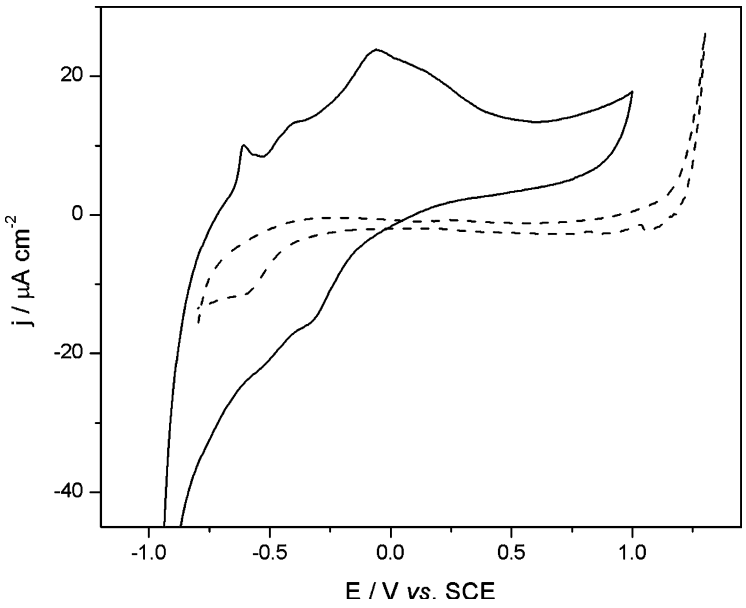

Fig. 1. Cyclic voltammetry of the SAE 1010 steel electrode in 0.7 M $NaNO_3$ (solid line) and in 0.10 M calcium benzoate + 0.7 M $NaNO_3$ (dashed line). Scan rate = 0.50 V min^{-1}. Temperature = 20 °C.

Fig. 2a corresponds to the SEM micrograph of the steel surface after 48 h in contact with sodium nitrate. A compact oxide layer with a smooth morphology, as well as residues of flower-like and quasi-globular oxides, developed on the steel surface. The structure of the globular formations can be seen with some detail in Fig. 2b. The

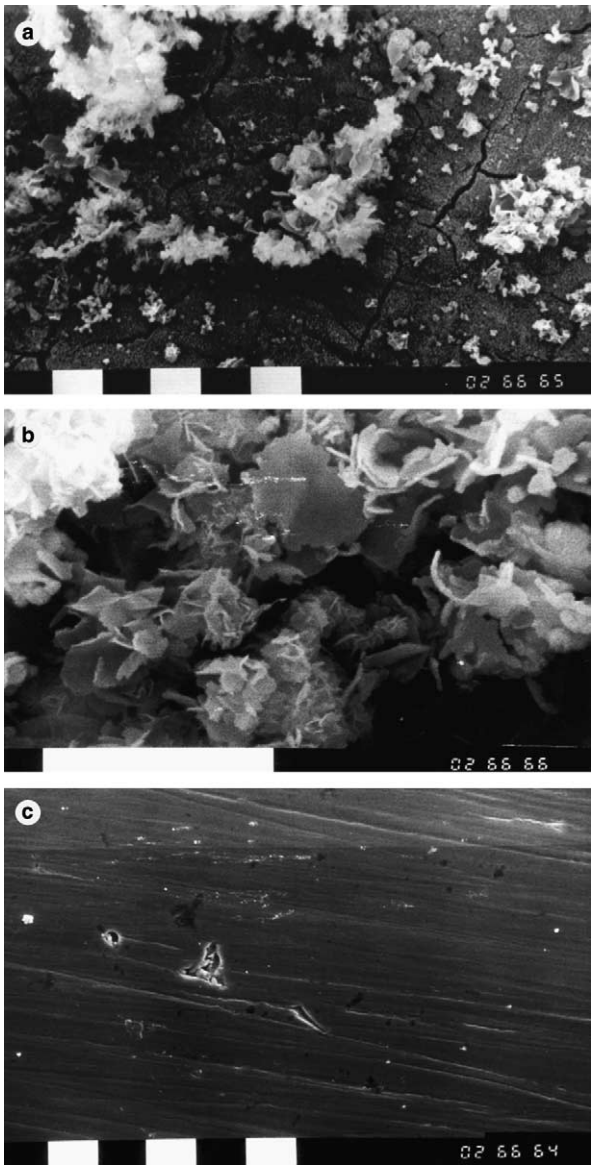

Fig. 2. SEM micrographs of a SAE 1010 steel surface put in contact with different electrolyte solutions during 48 h. (a) 0.70 M $NaNO_3$ (magnification 1000×), (b) 0.70 M $NaNO_3$ (magnification 5000×) and (c) 0.10 M calcium benzoate + 0.7 M $NaNO_3$ (magnification 1000×).

EDAX analysis revealed that the layer was basically composed by iron oxides. It was not possible to obtain more information with EDAX analysis in our case.

When calcium benzoate was added to the sodium nitrate solution, no signs of the globular oxide appeared after 48 h of exposure. A very smooth and, maybe, thin layer developed on the steel surface rendering it in the passive state (Fig. 2c). No significant amounts of calcium were detected on the surface by EDAX analysis.

The UV–visible reflectance spectrum of a steel panel (Fig. 3) in contact with the sodium nitrate solution depicted the characteristic absorption bands of iron oxides at 300–400 nm and at approximately ~500 nm [44–46]. On the other hand, the spectrum corresponding to the panel passivated by calcium benzoate showed a band approximately ~220 nm (Fig. 3), which was reported as a carbonyl group linked to the benzene ring into benzoate compounds [47].

3.2. Adsorption isotherms for benzoate on SAE 1010 steel in sodium nitrate solutions

3.2.1. Polarisation curves of steel in benzoate containing solutions

A PC of a SAE 1010 steel electrode was run at 0.05 V min^{-1} in oxygenated solutions with different concentrations of calcium benzoate (10^{-5}–10^{-1} M) + 0.70 M sodium nitrate without forced convection. Fig. 4 shows the PCs as log$j$ vs. E curves

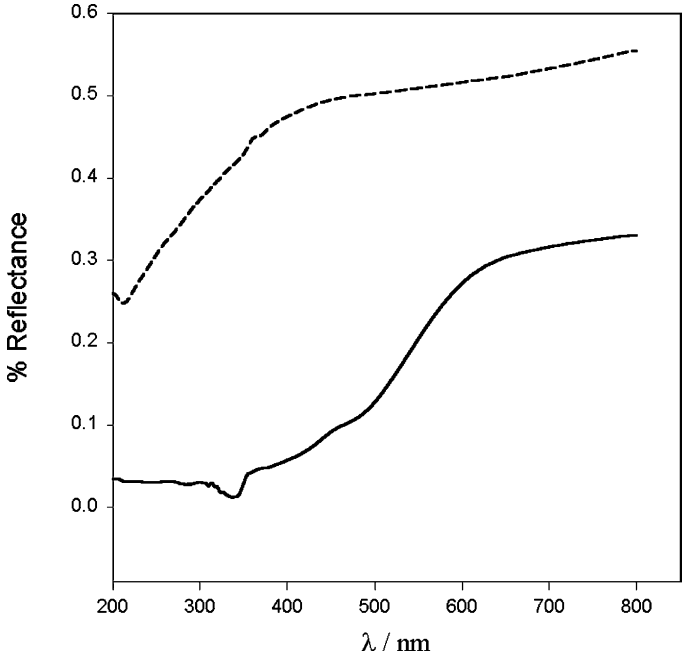

Fig. 3. UV–visible reflectance spectrum of a SAE 1010 steel surface put in contact with different electrolyte solutions during 48 h. (solid line) 0.70 M $NaNO_3$ and (dashed line) 0.10 M calcium benzoate + 0.7 M $NaNO_3$. Temperature = 20 °C.

in the presence of calcium benzoate. Table 1 shows the corrosion parameters, j_{corr}, and E_{corr}, together with the resulting values of θ, calculated according to Eq. (1) at $t_{ads} = 20$ min.

It can be clearly seen that for increasing benzoate concentrations, the values of j_{corr} decrease monotonously and at $C = 10^{-1}$ M a similar j_{corr} value results to that obtained when using $C = 10^{-2}$ M. In the case of E_{corr}, the tendency is to become more positive for increasing C values, clearly denoting the protection of the metal. Concomitantly, θ increased up to 93% for the most concentrated solution.

On the other hand, Table 2 exhibits another view to the inhibition process. Values of j_{corr} decrease for increasing t_{ads} values at oc conditions when using $C = 10^{-2}$ M in 0.70 M sodium nitrate. Moreover, θ matched 90% after 30 min of exposure and reached its maximum value (93%) 30 min later. These data clearly denote the inhibition of steel corrosion under the experimental conditions.

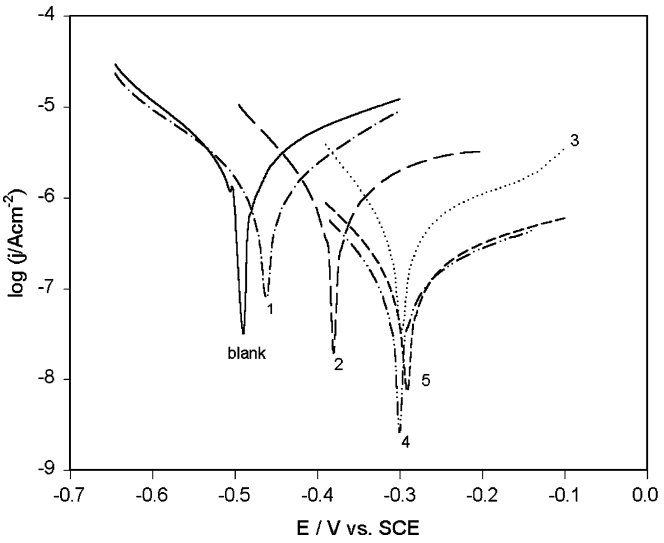

Fig. 4. log$j$ vs. E plots of a SAE 1010 steel electrode run at 0.05 V min^{-1} in 0.7 M $NaNO_3$ (solid line as blank) containing different concentrations of calcium benzoate; (1) 10^{-5} M (dashed dotted line); (2) 10^{-4} M (long dashed line); (3) 10^{-3} M (dotted line); (4) 10^{-2} M (dashed doubled dotted line); (5) 10^{-1} M (short dashed line). Temperature = 20 °C. Unstirred solutions.

Table 1
Corrosion parameters and degree of coverage by benzoate on SAE 1010 steel in 0.7 M $NaNO_3$ containing different concentrations of calcium benzoate for 20 min and 20 °C

C (M)	E_{corr} (V vs. SCE)	j_{corr} (nA cm^{-2})	θ (%)
0	−0.488	575	–
10^{-5}	−0.463	407	29
10^{-4}	−0.379	229	60
10^{-3}	−0.298	173	70
10^{-2}	−0.303	44	92
10^{-1}	−0.286	39	93

Table 2
Corrosion current densities and surface coverage values by benzoate for a SAE 1010 steel electrode as a function of time (t_{ads})

t_{ads} (min)	j_{corr} ($nA\,cm^{-2}$)	θ (%)
0	176	–
5	139	21
10	99	43
15	58	67
20	45	89
30	23	90
45	15	91
60	12	93

The coverage (θ) was determined at the open circuit potential in 0.01 M calcium benzoate + 0.7 M $NaNO_3$ at 20 °C.

The dependence of θ as a function of t_{ads} can be explained from data of Table 2. For $t_{ads} < 30$ min θ increases fast with time, whereas for $t_{ads} > 30$ min, the surface coverage reaches a limiting *plateau* value (93%). This behaviour can be explained considering another type of adsorption configuration for the molecule. However, a change in the functional group attachment upon adsorption is not really expected when varying the potential value, i.e., from the carboxylate or the aromatic ring towards steel [48]. The interaction between π bonding states of the aromatic ring with noble metal surfaces has been extensively studied in the case of thin-layer electrochemical interfaces. At potentials larger than that of zero charge of the interface, the aromatic compounds (containing different functional groups) are adsorbed with the phenolic ring parallel to the surface at low concentrations [48]. At these potentials the interaction between the π bonds of the molecule and d_z^2 orbital of the metallic atoms are strong enough to stabilise the adsorbed residue without any oxidative disruption [48,49]. On the other hand, when the surface concentration is high enough, the re-orientation of the aromatic ring being normal to the surface takes place [49]. In our case, a similar interaction between benzoate and steel is expected for low surface concentrations of iron oxides.

3.2.2. Evaluation of the adsorption isotherms of benzoate on SAE 1010 steel in sodium nitrate

The values of θ can also depend on the values of E_{ads}, thus, the influence of the electrode potential to benzoate adsorption was studied at a fixed $t_{ads} = 30$ min, where a plateau is reached.

Values of j_{corr} were calculated at different E_{ads} according to Section 2. When $E_{ads} <$ oc, the values of j_{corr} are larger than those found at oc and when $E_{ads} \geqslant$ oc, almost constant values for j_{corr} are reached. It can be concluded that the optimum value of E_{ads} for benzoate adsorption is the oc potential. At the maximum benzoate coverage, a flat configuration parallel to the surface is expected as explained above. It involves the largest interaction of the two functional groups with the surface, i.e., carboxylate and aromatic ring moieties.

Different types of simple isotherms were assayed to evaluate the best fit of the experimental data. The values of θ used for the fitting procedure correspond to the oc potential at t_{ads} = 20 min. The equation obeying those isotherms can be gathered in;

$$\frac{\vartheta}{(1-\vartheta)} = KC\exp(-r\vartheta) \tag{2}$$

where $K = (1/55.5)\exp(-\Delta\overline{G}^0_{ads}/RT)$ being $\Delta\overline{G}^0_{ads}$ the electrochemical standard free energy of adsorption by benzoate on steel. The value "55.5" denotes the molar concentration of the water displaced by benzoate species at the surface and r is the lateral interaction parameter for the adsorption process. The rest of the symbols have their usual meanings.

A Langmuirian behaviour is observed ($r = 0$), since a linear $\ln(\theta/1-\theta)$ vs. $\ln C$ plot was obtained (Fig. 5). Then, the equation representing benzoate adsorption on steel is

$$\frac{\vartheta}{(1-\vartheta)} = (C/55.5)\exp\left(\frac{-\overline{\Delta G^0_{ads}}}{RT}\right) \tag{3}$$

Considering Eq. (3) the value of $\Delta\overline{G}^0_{ads} = -32\ \mathrm{kJ\,mol^{-1}}$ was found, showing a large stabilisation of the inhibitor on the steel surface at the oc potential.

3.3. The effect of chloride on steel in nitrate solutions containing benzoate

Fig. 6 depict linear PCs on a SAE 1010 steel surface in 0.01 M, 0.10 M and 0.40 M sodium chloride solution run from −1.00 V to 0.20 V. The interface has been previously left in contact with a 0.10 M benzoate-containing solution at oc during 30 min.

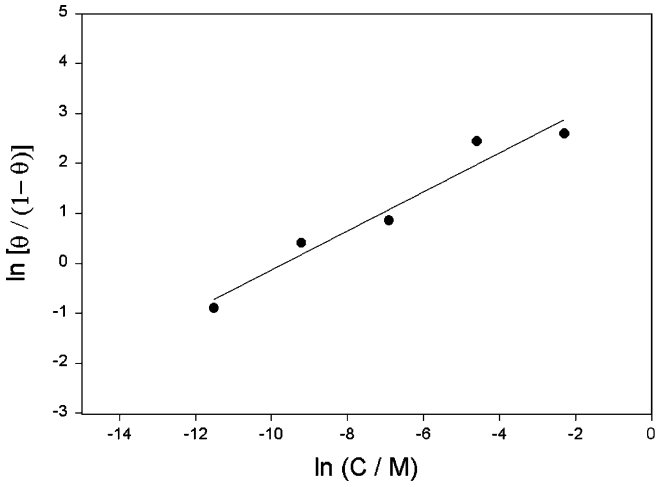

Fig. 5. Adsorption isotherm of calcium benzoate on SAE 1010 steel for a Langmuirian behaviour depicted as $\ln(\theta/1-\theta)$ vs. $\ln C$ plot. The open circuit potential is used for 30 min of adsorption in 10^{-2} M calcium benzoate + 0.70 M $NaNO_3$. Temperature = 20 °C. Unstirred solutions.

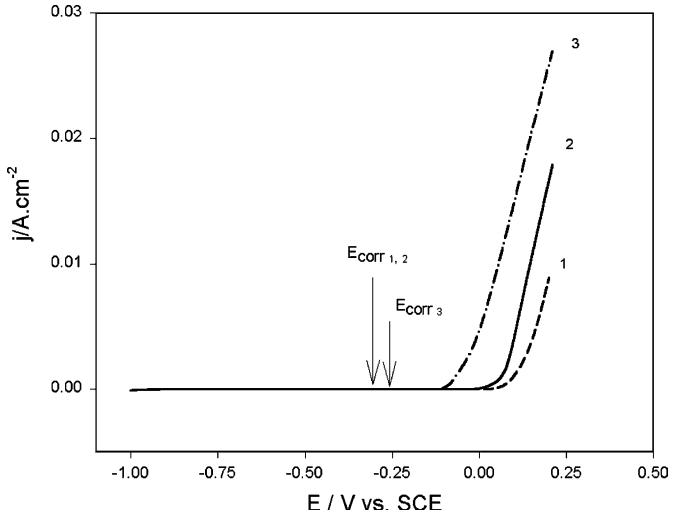

Fig. 6. Linear polarisation curves of a SAE 1010 steel electrode run at 0.05 V min^{-1} in different NaCl concentrations; (1) 0.01 M (dashed line); (2) 0.10 M (solid line); (3) 0.40 M (dotted dashed line). The electrode surface has been left during 30 min at the open circuit potential in 0.10 M calcium benzoate + 0.70 M $NaNO_3$. $E_{corr1,2}$ and E_{corr3} are the corrosion potentials in 0.01, 0.10 and 0.40 M NaCl, respectively.

Calculated E_{corr} values are similar for 0.01 M and 0.10 M, i.e., −0.30 V. However, when sodium chloride concentration is increased to 0.40 M, $E_{corr} = -0.25$ V. Fig. 6 also exhibits pitting potentials as the abscissa to the sudden increase in the current intensities. The increase in the chloride concentration produces the proximity between pitting and corrosion potentials.

3.3.1. The influence of chloride on steel using Routine A

Fig. 7 shows the log$j$ vs. E plots for the steel surface treated according to *Routine A*. Benzoate was adsorbed on the electrode at oc potential in two different situations. On one hand, the surface with the benzoate residue was put in contact with different sodium chloride concentrations (0.01 M, 0.10 M and 0.40 M). On the other hand, the electrode was immersed in the same sodium chloride concentrations but in the presence of 0.10 M calcium benzoate. In order to interpret the experimental results with *Routine A*, a blank experiment was also performed without adding calcium benzoate to any testing solutions.

It has been found from the above figure that at sodium chloride concentrations higher than 0.10 M, the inhibitor layer is slightly altered by the pitting agent. In this sense, the values of E_{corr} change from −0.283 V to −0.248 V, when the chloride concentration is increased from 0.10 to 0.40 M (plots (2) and (3)). However, there are small changes when a similar experiment is conducted with calcium benzoate in solution together with sodium chloride. For example, E_{corr} varies from −0.520 V to −0.496 V, when the chloride concentration is increased from 0.10 to 0.40 M (plots (2′) and (3′)). Evidently, when the experiments above are compared between each

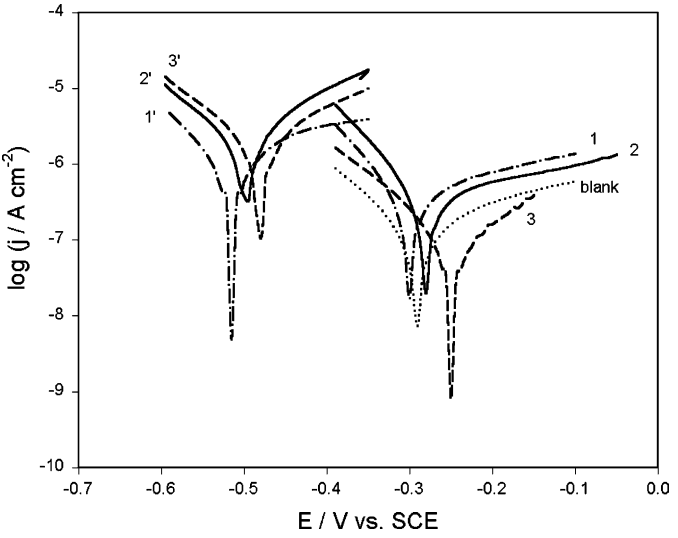

Fig. 7. log$j$ vs. E plots of a SAE 1010 steel electrode run at 0.05 V min^{-1} in solutions containing 0.10 M calcium benzoate + 0.70 M $NaNO_3$ + NaCl of (1) 0.01 M (dashed dotted line); (2) 0.10 M (solid line); (3) 0.40 M (dashed line). log$j$ vs. E plots of a SAE 1010 steel electrode run at 0.05 V min^{-1} in 0.70 M $NaNO_3$ with different NaCl concentrations; (1′) 0.01 M (dashed dotted line); (2′) 0.10 M (solid line); (3′) 0.40 M (dashed line). The electrode was previously conditioned according to *Routine A*. A blank experiment (dotted line) without growing a benzoate layer is also indicated.

other (similar chloride concentrations) E_{corr} values are always approximately 0.2 V more positive in the presence of solution benzoate than in the absence. This means that the first layer of the inhibitor (*Routine A*) grown at oc potential for 30 min has a profound effect upon corrosion. Besides, the inhibitor layer can be continuously grown even in the presence of chloride. This can be better seen through j_{corr} values. For example, comparing at 0.10 M sodium chloride the experiments run without calcium benzoate in solution (plot 2′), $j_{corr} = 316\,nA\,cm^{-2}$, whereas in the presence of 0.10 M calcium benzoate (plot 2); $j_{corr} = 16\,nA\,cm^{-2}$. Also, in a more concentrated sodium chloride solution (0.40 M) j_{corr} values decrease from 100 to $1\,nA\,cm^{-2}$, due to the lower oxygen solubility in the large-ionic-strength electrolyte (higher than 1.2 M). This behaviour is not expected but it has been found in other reports [25]. It was explained from the decrease of the mass transfer current density with the solubility and diffusion coefficient of soluble oxygen.

3.3.2. The influence of chloride in comparison with results from Routine B

The formation of a steel pre-passivated layer previous to the study of the inhibition of benzoate in the presence of sodium chloride (0.40 M) is analysed in this section. In order to compare corrosion parameters, the same routine was performed in two different cases; firstly without the inhibitor and secondly without the pitting agent. Fig. 8 shows the log$j$ vs. E plots for *Routine B* in which the surface is subjected to a 0.40 V potential in the two cases pointed above. This figure compares the effect

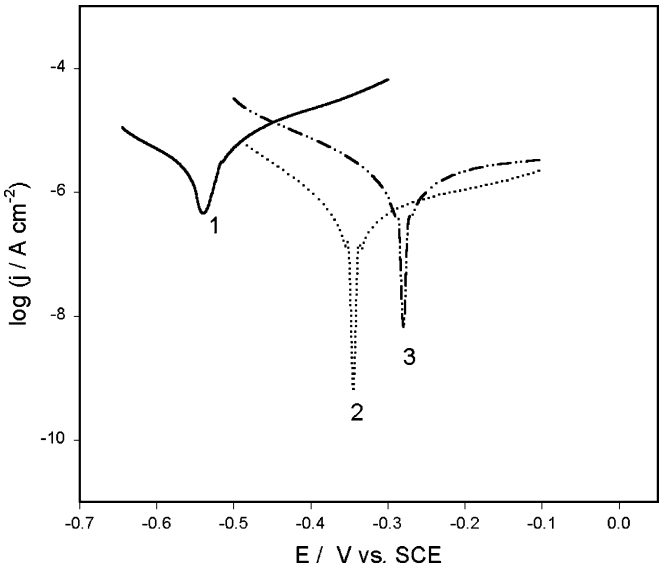

Fig. 8. log$j$ vs. E plots of a SAE 1010 steel run at 0.05 V min^{-1} according to *Routine B*. Polarisation curves were run in the following conditions: (1) 30 min in 0.70 M $NaNO_3$ followed by 10 min at 0.40 V and 10 min in 0.40 M NaCl (solid line); (2) 30 min in 0.10 M calcium benzoate + 0.70 M $NaNO_3$ followed by 10 min at 0.40 V and 10 min in 0.40 M NaCl (dotted line); (3) 30 min in 0.10 M calcium benzoate + 0.70 M $NaNO_3$ followed by 10 min at 0.40 V (double dotted dashed line).

of chloride after passivation in the presence (dotted line, 2) and in the absence (solid line, 1) of the inhibitor. The calculation of corrosion parameters shows a 0.25 V potential shift of E_{corr} to more positive values in the experiment with the inhibitor, and also two orders of magnitude lower j_{corr} values, i.e., from 320 to 0.7 nA cm^{-2}. On the other hand, when no chloride is put in contact with the passivated steel surface after the inhibitor adsorption, the values of E_{corr} are even more stable, that is, -0.282 V, with $j_{corr} = 4.0$ nA cm^{-2}.

In conclusion we can say that the inhibitor remained on the steel surface even after passivation, causing a lower value of j_{corr}. This is an important feature because passivation and inhibition processes in many cases show opposite results.

On the other hand, when performing the same experiment with 0.40 M of chloride after 24 h of resident time, the values $E_{corr} = -0.65$ V and $j_{corr} = 4.4$ μA cm^{-2} are obtained. These corrosion parameters mean large activities, so the long-term exposure experiments failed in the presence of chloride.

4. Conclusions

1. The voltammetric profile of steel in calcium benzoate solutions showed little activation by iron dissolution, thus pointing out the inhibitive action of calcium benzoate.

2. The maximum surface coverage degree by calcium benzoate was found to be 0.93 after 30 min.
3. The adsorption of calcium benzoate on SAE 1010 steel electrode was found to be of a Langmuirian type. The calculated value of $\Delta\overline{G}^{0}_{ads}$ was $-32\,kJ\,mol^{-1}$, showing a large stabilisation of the inhibitor on the steel surface.
4. In order to achieve better results, the suggested concentration of the inhibitor on steel lies between 10^{-2} M and 10^{-1} M.
5. The best performance of the inhibitor was found to occur at the open circuit potential. The increase of the electrode potential produced a fast increase in the corrosion current density.
6. The presence of chloride had a deleterious effect on the protective properties of calcium benzoate either on the surface or in solution.

Acknowledgments

We want to thank CIC (Comisión de Investigaciones Científicas de la Provincia de Buenos Aires-Argentina), UNLP (Universidad Nacional de La Plata) and Universidad de la República of Uruguay for their financial support. G.B. also thanks RELACQ for the fellowship granted.

References

[1] H.H. Uhlig (Ed.), The Corrosion Handbook, J. Wiley and Sons Inc., USA, 1948, pp. 125–207.
[2] L.L. Shreir (Ed.), Corrosion, Corrosion Control, Vol. 2, Newnes-Butherworths, England, 1976 (Chapter 18).
[3] W. Flick, Corrosion Inhibition. An Industrial Guide, second ed., Noyes Publications, USA, 1993.
[4] H. Kaesche, Metallic Corrosion. Principles of Physical Chemistry and Current Problems, An official NACE Publication, Houston, TX, 1985 (Chapter 7).
[5] I.L. Rozenfeld (Ed.), Corrosion Inhibitors, McGraw-Hill, New York, 1981.
[6] G. Trabanelli, V. Carasetti, in: M.G. Fontana, R.W. Staehle (Eds.), Advances in Corrosion Science and Technology, Vol. 1, Plenum Press, New York, 1970, p. 147.
[7] S.L. Granese, B.M. Rosales, C. Oviedo, J.O. Zerbino, Corros. Sci. 33 (1992) 1439.
[8] F. Bentiss, M. Lagrenee, M. Traisnel, J.C. Hornez, Corrosion (NACE) 55 (1999) 968.
[9] R. Manickvasagam, K. Jeyakarthic, M. Paramasivam, S. Venkatakrishna Iyer, Anti-Corros. Methods Mater. 49 (2002) 19.
[10] M.N. Desai, M.B. Desai, Corros. Sci. 24 (1984) 649.
[11] M. Abdallah, A.A. El-Sarawy, A.Z. El-Sonbati, Corros. Prev. Control 48 (2001) 97.
[12] T. Szauer, Z. Klenowicz, Z. Szlarska-Smialowska, Corrosion (NACE) 36 (1980) 400.
[13] M. Metikos-Hukovic, R. Babic, Z. Grubac, S. Brinic, J. Appl. Electrochem. 26 (1996) 443.
[14] B. Donelly, T.C. Downie, R. Grehowiak, D. Short, Corros. Sci. 14 (1974) 597.
[15] J.C. Lin, S.L. Chang, S.L. Lee, J. Appl. Electrochem. 29 (1999) 911.
[16] A. Singh, R.S. Chaudhary, Brit. Corros. J. 31 (1996) 300.
[17] R. Agrawal, T.K.G. Namboodhiri, J. Appl. Electrochem. 27 (1997) 1265.
[18] M.A. Quraishi, J. Rawat, M. Ajmal, Corrosion (NACE) 54 (1998) 996.
[19] M.G. Fontana, N.D. Greene, Corrosion Engineering, McGraw-Hill Book Company, USA, 1978, Chapter 6, pp. 200–202.

[20] M. Amalhay, I. Ignatiadis, in: P.L. Bonora, F. Deflorian (Eds.), Electrochemical Methods in Corrosion Research, Vols. I and II, Mater. Sci. Forum 289–292 (1998) 169–180.
[21] M.W. Kendig, A.T. Allen, S.C. Jeanjaquet, F. Mansfeld, in: R. Baboian (Ed.), Electrochemical Techniques for Corrosion Engineering, An official NACE Publication, Houston, TX, 1986, pp. 151–160.
[22] G.R. Cameron, A.S. Chiu, in: R. Baboian (Ed.), Electrochemical Techniques for Corrosion Engineering, An Official NACE Publication, Houston, TX, 1986, pp. 183–189.
[23] J.O'M. Bockris, M.A. Habib, J.L. Carbajal, J. Electroanal. Chem. 131 (1993) 81.
[24] B.R. Sharifker, M.A. Habib, J.L. Carbajal, J.O'M. Bockris, Surf. Sci. 173 (1986) 97.
[25] D. Eurof Davies, Q.J.M. Slaiman, Corros. Sci. 13 (1973) 891.
[26] D. Eurof Davies, Q.J.M. Slaiman, Corros. Sci. 11 (1971) 671.
[27] P. Agarwal, D. Landolt, Corros. Sci. 40 (1998) 673.
[28] C.-O.A. Olson, P. Agarwal, M. Frey, D. Landolt, Corros. Sci. 42 (2000) 1197.
[29] O. Lahodny-Šarc, F. Kapor, Mater. Sci. Forum 289–292 (1998) 1205.
[30] D.S. Azambuja, L.R. Holzle, I.L. Muller, C.M.S. Piatnicki, Corros. Sci. 41 (1999) 2083.
[31] P.N.S. Yadav, A.K. Singh, R. Wadhwani, Corrosion (NACE) 55 (1999) 937.
[32] V.S. Muralidharan, R. Sethuraman, S. Krishnamoorthy, Bull. Electrochem. 4 (1988) 705.
[33] A.K. Mohamed, S.A. Abd El-Maksoud, A.S. Fonda, Portug. Electrochim. Acta 15 (1997) 27.
[34] I.A. Raspini, Corrosion (NACE) 49 (1999) 821.
[35] B. Sanyal, Prog. Org. Coat. 9 (1981) 166.
[36] S.A. Hodges, W.M. Uphues, M.T. Tran, Surf. Coat. Int. 80 (1997) 178.
[37] D. Darling, R. Rakshpal, Mater. Perform. 37 (12) (1998) 42.
[38] E. Śmieszek, M. Zubielewicz, Farbe & Lack 102 (1996) 81.
[39] A. Braig, Prog. Org. Coat. 34 (1998) 13.
[40] H. Leidheiser Jr., JCT 53 678 (1981) 29.
[41] Z. Szklarska-Smialowska, J. Mankowsky, Brit. Corros. J. 4 (1969) 271.
[42] S. Gee, Surf. Coat. Int. 80 (1997) 316.
[43] J.O. Zerbino, J.R. Vilche, J. Appl. Electrochem. 11 (1981) 703.
[44] C.A. Borrás, R. Romagnoli, R.O. Lezna, Electrochim. Acta 45 (2000) 1717.
[45] G. Kortüm, Reflectance Spectroscopy, Springer-Verlag, New York, 1969.
[46] G. Larramona, C. Gutiérrez, J. Electrochem. Soc. 136 (1981) 2171.
[47] J.W. Cooper, Spectroscopic Techniques for Organic Chemists, A Wiley-Interscience Publication, J. Wiley and Sons, USA, 1980, pp. 67–69, 110.
[48] M.P. Soriaga, P.H. Wilson, A.T. Hubbard, J. Electroanal. Chem. 142 (1982) 317.
[49] V. Chia, J.H. White, M.P. Soriaga, A.T. Hubbard, J. Electroanal. Chem. 217 (1987) 121.
[50] W.W. Frenier, F.B. Growcock, V.R. Lopp, Corrosion (NACE) 44 (9) (1988) 590.